H. ZHOU[a], H. FANG[a, b], Q. ZHANG[c], Q. WANG[c], C. CHEN[d], S. J. MOONEY[e], X. PENG[a] & Z. DU[c]

[a] *State Key Laboratory of Soil and Sustainable Agriculture, Institute of Soil Sciences, Chinese Academy of Sciences. No. 71 East Beijing Road, Nanjing 210008, P.R. China,* [b]*University of Chinese Academy of Sciences, No.19A Yuquan Road, Beijing 100049, China,* [c]*Institute of Environment and Sustainable Development in Agriculture, Chinese Academy of Agricultural Sciences, No. 12 Zhongguancun South Steet, Haidian District, Beijing, 100081, P.R. China,* [d]*Department of Soil and Water Sciences, China Agricultural University, No. 2, Yuan Ming Yuan Xi Lu, Beijing 100193, China, and* [e]*Division of Agricultural and Environmental Sciences, School of Biosciences, University of Nottingham, Sutton Bonington Campus, Loughborough, Leicestershire LE12 5RD, UK.*

Correspondence: Z. Du. Email: duzhangliu@caas.cn

Running title: Biochar effects on soil hydraulic function and aggregation

Summary

Biochar has the potential to modify soil structure and soil hydraulic properties because of its small particle density, highly porous structure, grain size distribution and surface chemistry. However, knowledge of the long-term effects of biochar on soil physical properties under field conditions is limited. Using an 8-year field trial, we investigated the effect of successive additions of high-dose maize cob-derived biochar (9.0 t ha^{-1} year^{-1}, HB), low-dose maize cob-derived biochar (4.5 t ha^{-1}

This article has been accepted for publication and undergone full peer review but has not been through the copyediting, typesetting, pagination and proofreading process, which may lead to differences between this version and the Version of Record. Please cite this article as doi: 10.1111/ejss.12732

year^{-1}, LB), straw return (SR) and control (no biochar or straw, CK) on soil aggregate distribution, three-dimensional (3-D) pore structure, hydraulic conductivity and water retention in the upper 10 cm of a sandy loam soil from the North China Plain. Results showed that LB and HB treatments increased soil organic C content by 61.0–116.3% relative to CK. Interestingly, biochar amendment did not enhance the proportion of macroaggregates (>2 and 0.25–2 mm) or aggregate stability, indicating limited positive effects on soil aggregation. The HB treatment decreased soil bulk density, increased total porosity and macroporosity (>30 μm). The retention of soil water, including gravitational water (0–33 kPa), capillary water (33–3100 kPa) and hygroscopic water (> 3100 kPa), were all improved under HB soil. The HB and LB treatments increased plant available water content by 17.8 and 10.1%, respectively, more than that of CK. In contrast, SR showed no significant increase in soil porosity and water retention capacity but improved the water stability of macroaggregates. We concluded that biochar used in the coarse-textured soil enhanced saturated hydraulic conductivity and water-holding capacity, but did not improve soil aggregation.

Key Words: Soil water retention curve, soil structure, pore-size distribution, X-ray microtomography

Highlights

- Pore structure and hydraulic properties were studied in an 8-year biochar-amended sandy loam.
- HB (high-dose biochar) increased total soil porosity and CT-identified macroporosity (>30 μm).
- Water retention improved under HB soil.
- Biochar addition had no effect on the formation of macroaggregate.

Introduction

Biochar has two typical characteristics: it is rich in organic carbon and has a highly porous structure (Lehmann & Joseph, 2015). The organic carbon compounds of biochar are very stable, and its potential to increase carbon sequestration has been extensively studied (Lehmann, 2007; Lehmann & Joseph, 2015). The porous structure of biochar, on the other hand, suggests that biochar has the potential to improve soil physical properties such as increasing porosity and water retention capacity (Blanco-Canqui, 2017). Recently, the feasibility of using biochar in agricultural fields has gained much interest in agricultural regions where water is scarce or under unfavourable soil structure conditions (Basso *et al*., 2013).

Previous research has reported positive effects of biochar from different sources on the physical properties of soils of various textures (e.g. sand, loamy sand, sandy loam, silt loam, clay) because of the highly porous structure and large specific surface area of biochar (Basso *et al*., 2013; Lu *et al*., 2014; Burrell *et al*., 2016; Petersen *et al*., 2016). Biochar is considered to decrease soil bulk density and increase soil porosity (Basso *et al*., 2013; Burrell *et al*., 2016; Petersen *et al*., 2016), which consequently enhances hydraulic conductivity (Devereaux *et al*., 2012; Lim *et al*., 2016) and soil water retention (Castellini *et al*., 2015; Burrell *et al*., 2016). Biochar from wood and wheat straw are also reported to improve the pore system and water retention of coarse textured soils (sandy loam and loamy sand soils) indirectly by increasing root growth and soil organic carbon (SOC) sequestration (Devereaux *et al*., 2012; Bruun *et al*., 2014). The increase of SOC by straw and wood biochar was also reported to increased soil aggregation of clay soil (Sun & Lu, 2014). However, many studies also found that biochar has negligible or even negative effects on soil physical properties. Peng *et al*. (2011) and Rahman *et al*. (2017)

have shown that the amendment of straw biochar had no effect on the water stability of clay soil. The reduced soil structural stability after adding biochar may be ascribed to increased clay dispersibility through its influence on soil pH, ionic strength, zeta potential and moisture content (Khademalrasoul *et al*., 2014; Amoakwah *et al*., 2017a). Hardie *et al*. (2014) also found that water retention of a sandy loam was not affected by biochar from tree waste.

The inconsistent effects of biochar can be attributed to differences in the intrinsic attributes of different biochars (Castellini *et al*., 2015; Burrell *et al*., 2016; Wang *et al*., 2017) or to the soil properties it is mixed with (Castellini *et al*., 2015). For example, Suliman *et al.* (2017) found that maize straw biochar and beech wood biochar had different porosities and different surface functionalities, and they had clearly contrasting effects on the hydrologic properties of a sandy soil. Wang *et al*. (2017) reported that the effects of biochar (walnut shells and wood from coniferous trees) depended on soil texture, with improved aggregation in a silt loam but no effect on a sandy loam. In addition to the biochar and soil factors, there are two other important factors that might contribute to the inconsistent results. The first, suggested by Hardie *et al*. (2014), is that field and laboratory experiments are often not comparable. The role biochar plays in repacked and in structured soils varies greatly, especially if the biochar particle size and mixing ratios are different. A second aspect is the duration of the experiment. Most of the studies concerning biochar are conducted over a short term (e.g. < 2 years), especially those in the laboratory, while relatively few have been established for long-term assessment (e.g. > 5 years). Soil processes, for example soil aggregation, take place over long timescales, therefore, the effect of biochar in the short-term experiment might be different from those in long-term experiments. To gain a better understanding of the effects of biochar on the physical properties of agricultural soil, it is likely

that long-term field experiments are required (Blanco-Canqui, 2017).

Straw incorporation has been widely considered an environmentally friendly practice to maintain soil quality and increase crop yields in many agricultural regions. Straw can be also converted into biochar as a soil amendment to improve soil properties (Lehmann, 2007). It is well known that biochar is effective in enhancing the long-term SOC sequestration (Qayyum *et al.*, 2012). However, whether straw-derived biochar is more effective in improving soil physical properties remains unclear.

We established a field biochar experiment with annual biochar (from maize cobs, at 360°C) input in 2007 in a winter wheat (*Triticum aestivum* L.)–summer maize (*Zea mays* L.) double cropping system in the North China. In the last few years, biochar effects on enzyme activities (Du *et al.*, 2014) and SOC stabilization mechanisms (Du *et al.*, 2017) have been reported based on this field trial. However, there is a knowledge gap as to how biochar alters soil structure and the mechanisms responsible for hydraulic properties. Here, we hypothesized that long-term biochar application could modify soil pore structure and consequently affect soil water retention and hydraulic conductivity. The specific objectives were to evaluate the effects of biochar amendment on soil pore structure with X-ray computed tomography (CT) and the associated effects on water retention and hydraulic properties. The effect of straw incorporation was also evaluated.

Materials and Methods

Site description

This study was carried out on a sandy loam soil at the Huantai Agroecosystem Experimental Station (36° 57′ N, 117° 59′ E), Huantai County, Shandong province, China. The experimental site

is representative of the intensive agricultural areas of the North China Plain. The typical cropping system is a winter wheat–summer maize rotation. This site has a warm temperate continental monsoon climate, with the annual average temperature and precipitation of 12.4°C and 600 mm, respectively. The soil (Fluvic Cambisol) has 73.5% sand (0.05–2 mm), 12.5% silt (0.002–0.05 mm) and 14.0% clay (<0.002 mm) for the 0–20-cm depth.

Experimental design

The field experiment was established in 2007, including four treatments: control (no biochar or straw, CK), low-dose biochar (4.5 t ha^{-1} $year^{-1}$, LB), high-dose biochar (9.0 t ha^{-1} $year^{-1}$, HB) and straw return (SR). This trial was laid out as a randomized complete block design with three replications and each plot was 36 m^2. For the CK, LB and HB treatments, the aboveground wheat and maize straws after harvesting were removed from the field. Instead, all wheat and maize straws (~15 t ha^{-1} $year^{-1}$) in the SR treatment were returned to the fields annually. The conversion efficiency of straws into biochar through pyrolysis is about 30%. Thus, the biochar used in the LB treatment (~4.5 t ha^{-1} $year^{-1}$) was equivalent to the amount of biochar that can be produced by the straw used in the SR treatment. The HB treatment was incorporated with double the amount of biochar as in the LB treatment, i.e. 9.0 ha^{-1} $year^{-1}$. The biochar used in this study was produced by incomplete self-combustion of crushed maize cobs at 360°C for 24 hours by a local biochar company. The biochar had a pH of 8.2, and contained 65.7% C and 0.91% N. The mean size of biochar was 0.11 mm. These four treatments used the same amount and type of inorganic fertilizers (Du *et al.,* 2014). For each crop season, the N fertilizers as urea of 200 kg N ha^{-1}, P as superphosphate of 52.5 kg ha^{-1} and K as potassium sulphate of 37.5 kg K_2O ha^{-1}. The biochar and inorganic fertilizers were incorporated into the soil by rotary tillage (~16-cm depth) before each

crop season.

Sampling

Topsoil samples (0–100 mm) were collected before the harvest of wheat in May 2015. Three undisturbed 50-mm long soil cores (50-mm diameter, 50-mm long) were randomly sampled at the 25–75-mm depth with polyvinyl chloride (PVC) rings from each plot for measuring soil bulk density (ρ_b), water content and saturated hydraulic conductivity (K_s) and X-ray CT scanning. Three undisturbed 25-mm long soil cores were collected from the 30-60-mm depth with small-sized steel rings (50-mm diameter, 25-mm long) for determining the soil water retention curve (SWRC). Soil cores were wrapped with plastic films to prevent water evaporation. Five bulk samples were also collected from the 0–100-mm depth from each plot with a shovel and then were pooled together to make one bulk sample. All the sampling was undertaken in the inter-row of the wheat crop. Care was taken to avoid disturbing soil structure during sampling and transport. Samples were stored in refrigerator at 4 °C before measurement.

X-ray microtomography (μ-CT) scanning and image analysis

The 50-mm-long soil cores were scanned at field moisture conditions with an industrial Phoenix Nanotom X-ray μ-CT (GE, Sensing and Inspection Technologies, GmbH, Wunstorf, Germany). Detailed settings of the scanning and image analysis can be found in Zhou *et al*. (2016). Briefly, samples were scanned at a voltage and a current of 110 kV and 100 μA, respectively. The image reconstruction was conducted using the Datos|x 2.0 software and generated a stack of 1700 slices. Each slice had a size of 1700 × 1700 voxels with each voxel representing a volume of 0.03 mm × 0.03 mm × 0.03 mm. The next step in the image analysis was to select a 3-D region of interest (ROI), with the size of 1000 × 1000 × 1500 voxels from the centre of the cores. The selected

grayscale images were preprocessed by enhancing the contrast and filtering with a median filter (2 x 2 x 2) using the ImageJ software (Rasband, 2007). A bi-level method (Vogel & Kretzschmar, 1996) was used for the image segmentation. Image-based macroporosity was calculated as the ratio between the volume of pores and volume of the ROI. The morphological opening operation was used to determine pore-size distribution (PSD). Briefly, pores smaller than a spherical mask with a certain size were removed during the opening operation and their porosity can be determined. By successively increasing the size of the mask, PSD can be quantified. Image segmentation and quantification was implemented with the open-source software Quantim4 (http://www.ufz.de/index.php?en=39198, verified on 20-08-2018).

Laboratory measurements and analyses

The bulk samples were air-dried in the laboratory and divided evenly into two parts. One part was sieved manually to three fractions: 2–3, 0.25–2 and <0.25 mm. The water stability of aggregates was tested separately on the 2–3-mm and 0.25–2-mm fractions using the fast-wetting methods proposed by Le Bissonnais (1996). Briefly, aggregates were oven-dried at 40°C for 24 hours, and then approximately 5 g of aggregates (2–3 mm or 0.25–2 mm) were placed in a glass beaker filled with 0.05 l deionized water for 10 minutes. All of the wetted samples were transferred to another glass beaker and dried in the oven at 40°C for 24 hours. Alcohol was used during the transfer process to avoid further breakdown of aggregates. The samples were then sieved into 2–3, 1–2, 0.5–1, 0.25–0.5, 0.05–0.25 and <0.05-mm fractions using a set of sieves with apertures of 2, 1, 0.5, 0.25 and 0.05 mm, respectively. The weights of the different fractions were measured and their proportions were determined separately. The aggregate stability was expressed by the mean weight diameter (MWD), which is the summary of the products of each proportion of aggregate

fractions and the corresponding aggregate size (mean value of the apertures of the upper and lower sieves). The remaining part of the bulk samples was finely ground for the measurement of soil basic physicochemical properties. Soil organic carbon (SOC) content was determined using a CNS analyser (Vario Max CNS, Elementar, Hanau, Germany). Soil particle density (ρ_s) was determined by the pycnometer method (Blake & Hartge, 1986).

The 50-mm-long soil cores were unwrapped and weighed after CT scanning. Then they were slowly saturated and K_s was determined by the constant head method (Klute & Dirksen, 1986a). Then the soil cores were dried in the oven at 105 °C for 24 hours and weighed. Soil moisture at sampling was calculated from the dry weight and fresh weight of the cores. The ρ_b was determined from the dry weight and volume of the soil cores. Total porosity (ϕ) was calculated according to the relation: $\phi = 1 - \rho_b/\rho_s$.

The full range of SWRC, i.e. from saturation to dryness, was determined on the 25-mm-long soil cores. The wet region (0–1500 kPa) was measured by the sand box (0–10 kPa) and the pressure plate methods (10–1500 kPa) (Klute & Dirksen, 1986b). Gravitational water (0–33 kPa) was retained by macropores and was not available to plants. The relation between water content (θ) and water potential (ψ) for the wet region SWRC was fitted by the van Genuchten equation:

$$\theta = \theta_r + \frac{\theta_s - \theta_r}{[1+(\alpha\psi)^n]^m} \quad , \qquad (1)$$

where θ_s and θ_r are the saturated and residual soil water content, respectively. Alpha, n and m are shape parameters with $m = 1–1/n$. Plant available water was held mainly by capillary forces and plant available water content (PAWC) was determined as the difference between water content at field capacity (FC, 33 kPa) and plant permanent wilting point (PWP, 1500 kPa) (Cassel & Nielsen, 1986). The dry region SWRC (from 1500 kPa to oven dryness), which could indicate the ability

of soil to retain hygroscopic water (>3100 kPa), was determined by the adsorption method (Arthur *et al*., 2015). With this approach the SWRC does not continue over the whole range because the wet region was measured by the desorption approach. A detailed description of the method can be found in Chen *et al*. (2014). Previous studies have shown that the adsorption data of dry region SWRC followed a linear model, with the slopes (SL) indicating the ability of soil to retain hygroscopic water (Chen *et al*., 2014).

Statistical analysis

All statistical analyses were carried out with RStudio version 1.1.442 (RStudio Team, 2015). A one-way analysis of variance (ANOVA) with blocks was used to assess the effects of biochar and residue return on soil physicochemical properties, pore characteristics and hydraulic properties. The normality of residuals and assumptions of the homogeneity of variances were checked by the Shapiro–Wilk and Bartlett tests, respectively, for all analyses and data were transformed as necessary. Fisher's least significant difference (LSD) was used for multiple comparisons of means. Pearson correlation analysis was used to determine the relations between SOC and bulk density and SL. The variables included in the correlation analysis were tested for normality. The SOC, bulk density and SL were approximately normally distributed and no transformation was performed. A significance level of 0.05 was used throughout the study.

Results

General soil physiochemical properties

Relative to CK, biochar addition significantly increased SOC content by 61.0% under the LB and 116.3% under the HB treatments, whereas the difference between SR and CK was not significant (Table 1). Moreover, the SOC content increased with the rate of biochar application, showing that

the SOC content under HB treatment was larger by 34.4% than that of the LB treatment. Biochar addition or straw return had no significant effect on soil ρ_s (Table 1). Relative to the CK, the HB treatment significantly reduced ρ_b and increased ϕ, whereas the LB and SR treatments showed no significant difference (Table 1).

Aggregate size distribution and water stability

Aggregate size distributions determined by the dry sieving method are shown in Figure 1(a). The HB significantly reduced the proportion of >2 mm fraction by 32.0% and increased the <0.25 mm fraction by 161% relative to CK. However, there was no significant difference in aggregate-size distribution among the CK, LB and SR treatments (Figure 1).

The MWD of the water stable aggregates for the 2–3 mm and 0.25–2 mm aggregates after fast wetting (i.e. slaking) are presented in Figure 1(b). Straw return significantly increased the water stability of the 2–3 mm fraction by 29.6% compared with CK. However, biochar addition had no significant effect on the MWD of aggregates, although LB and HB had slightly larger MWD values (ranging from 0.235 to 0.247 mm) than that of CK (0.195 mm). For the 0.25–2 mm fraction, no significant difference in the water stability was observed among the treatments.

Soil macropore morphology and pore-size distribution

The 3-D macropore structures are shown in Figure 2. Visual observation showed that the HB treatment produced a greater number of pores and the SR treatment resulted in more large sized pores. Quantification of the 3-D pore system showed soil macroporosity followed the order SR > HB > SR, CK (Table 2), which was consistent with the visual observation. Specifically, HB and SR increased the soil macroporosity by 55.6 and 96.3% respectively relative to CK, though the difference between HB and CK was not significant (Table 2).

The pore-size distributions obtained from CT images with biochar additions are presented in Figure 3. No significant differences in the <0.3 and 0.3–1-mm size pores were found among treatments, although HB had slightly larger values than those of CK, LB and SR. For the >1-mm pores, SR and HB increased the porosity by 171 and 75.3%, respectively, compared to CK. We also observed limited changes in the porosity of the >1-mm pores between LB and CK treatments. These data suggested that straw return effectively increased the porosity of pores larger than 1 mm, but the effect of adding biochar, especially the low-dose biochar, was limited.

Soil water retention and saturated hydraulic conductivity

The wet region SWRCs were all well fitted by the van Genuchten equation (R^2 > 0.99) (Figure 4). Incorporation of biochar and straw generally increased soil water retention in the order of HB > LB and SR > CK, except for the near saturation range. Compared with CK, the HB and SR treatments significantly increased soil water retention capacity by 4.6 to 16.3% at suctions ≤30 kPa. The biochar and crop residue treatments enhanced water retention capacity by 5.1 to 16.1% over the CK treatment across the intermediate range of suction (30 to 300 kPa). At suctions between 500 and 1000 kPa, there was no significant change in water retention capacity among the treatments. As for the water retention characteristics, both FC and PWP followed the order of HB > LB >SR > CK (Table 2). For PAWC, the difference between FC and PWP was increased significantly by the incorporation of biochar (Table 2). The plant available water content (PAWC) under the HB and LH treatments was lager by 17.8 and 10.1%, respectively, than that of CK, but the difference between SR and CK was not significant.

Overall, the retention of adsorbed (hygroscopic) water was in the order of HB > LB > CK=SR (Figure 5), suggesting that biochar application increased soil water adsorption while straw return

did not. The data measured for each treatment were fitted with linear models ($R^2 > 0.98$) and their slopes (SL) indicate the ability of soil to retain hygroscopic water. The values of SL under HB were significantly larger by 8.0 and 7.9%, respectively, than those of the CK and SR treatments (Figure 6), indicating significantly greater water adsorption capability with a large biochar dose. However, the SL of the LB treatment showed no significant difference from the other treatments (Figure 6).

The effect of biochar addition on *K*s is shown in Table 2. Compared with the CK treatment, the HB treatments enhanced *K*s by 106.4%, whereas the LB and SR treatments showed no significant effect.

Discussion

Effects of biochar and straw incorporation on soil physiochemical properties

Biochar as a soil amendment has received much attention because of its capacity to alter many soil physical, chemical and biological properties (Blanco-Canqui, 2017). Our results showed clearly that the addition of biochar significantly decreased the ρ_b of the sandy loam studied (Table 1), which is consistent with previous studies on both fine (Castellini *et al.*, 2015) and coarse textured soils (Burrell *et al.*, 2016). The decrease in ρ_b after biochar incorporation partly relates to the smaller bulk density of the porous biochar (<0.6 g cm^{-3}) than of field soil (~1.2 g cm^{-3}) through the dilution effect. In addition, biochar can alter the packing of soil particles, and create additional external soil porosity (Lim *et al.*, 2016). There is also an assumption that biochar can reduce bulk density by interacting with soil particles and improving aggregation and thus porosity (Blanco-Canqui, 2017), however it was not tested in this study.

There was an increase in SOC after applying biochar in our study (Table 1) and many others irrespective of the type of biochar used (Arthur *et al.*, 2015; Fungo *et al.*, 2017). The linear

correlation between SOC content and soil ρ_b was significant and negative (r = –0.83, P < 0.001, Figure 7a), which accords with previous studies (Arthur *et al.*, 2015). Straw return, however, showed limited effects on SOC content and soil bulk density compared with biochar. A significant increase of SOC and decrease of bulk density with straw return have been reported (Lu *et al.*, 2009). The discrepancy with our study might be caused by the amount of straw and soil conditions. Overall, biochar application can increase SOC content and reduce bulk density, suggesting the potential to improve soil structural development and stability.

Effects of biochar and straw incorporation on aggregate size distribution and stability

Soil aggregation is an ecosystem process that leads to the formation and stabilization of soil structure, which consists of aggregates of different sizes and the generation of pore spaces. In the present study, adding biochar did not enhance the proportion of macroaggregates determined by the dry-sieving method. Instead, the HB treatment even significantly reduced the proportion >2 mm aggregates relative to the control (Figure 1). Previous research has also suggested that biochar can have mixed effects on aggregate size distribution (Blanco-Canqui, 2017). Positive effects of biochar on soil aggregation have been ascribed to the enhanced biotic contributions, including soil organic matter (SOM) and biological activities (Wang *et al.*, 2017). In this study, SOC increased after biochar application but did not contribute to soil aggregation, probably because SOC was stored predominantly in the form of free particulate C (Fungo *et al.*, 2017). It is well known that the organic C of biochar is recalcitrant and in is biologically less inactive and therefore less efficient in binding soil particles or promoting biological activities (Peng *et al.*, 2011).

Water stability of the macroaggregate fraction was not significantly improved by adding

biochar (Figure 1), indicating that biochar did not increase the binding agents to form stable macroaggregates. Similar results have been reported previously for an Ultisol amended with rice straw-derived biochar (Peng *et al.*, 2011). Positive effects of biochar from different sources on the aggregate stability of soil with different textures have been reported previously for both field and laboratory conditions as reviewed by Blanco-Canqui (2017). A recent study by Kumari *et al.* (2017) of the effect of birch wood-derived biochar on the dispersibility of colloids in sandy loam soil found the content of water-dispersible colloids increased with the rate of application of biochar. Consequently, the increase in clay dispersibility after biochar amendment might lead to a decrease in soil structural stability (Khademalrasoul *et al.*, 2014; Amoakwah *et al.,* 2017a). The inconsistent changes in the aggregate stability suggest that the effects of biochar are likely to be site-specific and involve many factors (e.g. biochar quality, clay dispersibility).

Straw incorporation significantly improved the water stability of macroaggregates, although SOM in the SR treatment increased only slightly (Figure 1; Table 1). This is consistent with Christensen (1986). In contrast to the stable nature of biochar, straws are easily decomposed and can release organic substances such as polysaccharides and organic acids, which could act as binding agents of soil particles (Degens, 1997). The fresh straw and the organic materials released also serve as the energy source for the growth of earthworms, fungi or microorganisms. The bioactivities of soil fauna and microorganisms and their exudates also contributed to soil aggregation. The different effects of biochar and straw on soil aggregation suggested that the organic C from straw decomposition or the microbial activity involved was effective in promoting soil aggregation, whereas the organic C of biochar was not.

Effect of biochar and straw incorporation on soil pore characteristics

Biochar application increased soil total porosity (Table 1), which is consistent with previous results from both incubation and field experiments on different soils (Basso *et al.*, 2013; Burrell *et al.*, 2016; Petersen *et al.*, 2016). The increase in total porosity is usually attributed to the low density and highly porous inner structure of biochar particles (Basso *et al.*, 2013; Petersen *et al.*, 2016), and their interaction with mineral soil particles (Blanco-Canqui, 2017). In addition, Hardie *et al.* (2014) proposed that the large macropores created in the soils surrounding biochar particles were another cause of increased total porosity. This assumption was further confirmed by the soil images from CT imaging, which showed that macropores were more evident in the HB treatment (Figure 2). The enhanced soil porosity after biochar addition consequently could have positive implications for the movement of water, heat and gases in the soil systems. However it should be noted that this is likely to depend on the ratio of biochar:soil. For example, Devereux *et al*. (2012) found that mean pore size reduced in soils with increased additions of biochar.

The size distribution of macropores identified by CT differed among the treatments. The SR and HB treatments had more >1 mm and 0.3–1 mm pores than CK (Figure 3), but the effect of the low-dose biochar was limited. Based on the total porosity and macroporosity data, we found that HB treatment significantly increased the <0.03 mm pores (those beyond the resolution of CT images). Petersen *et al.* (2016) recently reported that the wheat straw-derived biochar could convert drainage pores (60–300 μm) into the smaller water-holding pores (0.2–60 μm) in a coarse sandy soil. Lu *et al.* (2014) found that rice husk biochar increased the proportion of mesopores (6–45 μm) in an expanding clayey soil. More recently, Amoakwah *et al*. (2017b) reported that maize cob biochar increased the amount of micropores (< 3 μm) in an amended tropical sandy loam. These findings, together with our results, illustrate that the addition of biochar from different sources can modify

the pore system of soils with different textures. We suggest that these modifications are caused by the incorporation of biochar as a porous material, not by the alteration of soil aggregation processes because soil aggregation was not improved by biochar amendment in this study (Figure 1).

Effects of biochar and straw incorporation on soil hydraulic properties

Biochar can alter the soil pore system and therefore significantly influence soil hydrological function, which might result in changes in water cycling and ecosystem processes mediated by water. Correlation analysis showed *K*s values were positively correlated with 0.03–1-mm pores (r = 0.67, data not shown) but not with >1mm pores. This can be explained because the 0.03–1-mm pores are more continuous than the >1mm pores. In our study, high-dose biochar and straw incorporation increased the potential to store gravitational water (from saturation to 33 kPa, Figure 4), which can be explained by the increase in macroporosity (Table 2). However, this water is not available for plant growth. The increase of PAWC in the HB treatment indicated that soil micropores with equivalent diameter between 10 and 0.2 μm increased significantly with biochar amendment, which is consistent with Amoakwah *et al*. (2017b). We can attribute the increase in micropores to the porosity of biochar as discussed in the previous section (Basso *et al*., 2013). A significant increase in the retention of capillary water and PAWC was expected in the LB treatment with successive biochar amendment, but no significant increase was observed (Table 2). This indicated that the amount of biochar was an important controlling factor. Straw incorporation improved soil aggregation but did not improve the retention of capillary water (Figure 1; Table 2), probably because straw increased the number of macropores but not micropores (Figure 3).

Limited data are available about the effects of biochar on the hygroscopic water compared with the gravitational and capillary water. In this study, biochar significantly increased soil hygroscopic

water content (Figure 5), reflected by larger values of SL in the biochar amended soils over the control (Figure 6). We also found a positive correlation between SL and SOC content (Figure 7). It is likely because SOM is one of the key factors that determines surface properties of soils and sorption of water molecules, and the polar functional group on the biochar surface might serve as water adsorption cores and facilitate the formation of water clusters on the surface (Cybulak *et al.*, 2016). Our results are consistent with Arthur *et al.* (2015), who applied birch wood biochar on a sandy loam. Overall, we have shown that biochar addition can have positive effects on plant available and hygroscopic water under field experimental conditions.

Conclusions

Based on an 8-year field experiment, we found that successive high-dose biochar amendment on a sandy loam soil decreased soil bulk density and increased total porosity because of the highly porous structure of biochar. Biochar application increased SOC content, but did not improve soil aggregation. The retention of soil water, including gravitational, capillary and hygroscopic water, were all improved by incorporation of the large amount of biochar (HB). These improvements were attributed to the porous structure of biochar, but not to soil aggregation. These results suggest that biochar could be used in the agricultural soils with a coarse texture to improve soil porosity, enhance water-holding capacity and provide more plant available water. The lack of enhanced aggregation potential is a considerable limitation, however. In addition, such decisions on the incorporation of biochar should be taken in conjunction with information about the effects of biochar on soil biochemical characteristics.

Acknowledgements

This work was financially supported in part by the Special Fund for Agro-scientific Research in

the Public Interest (201503116), National Water Pollution Control and Treatment Science and Technology Major Project in China (2015ZX07103-007), the Chinese National Basic Research Program (2015CB150400), Natural Science Foundation in Beijing (6173035) and National Key Research and Development Program (2016YFD0300906). We appreciate the constructive comments of two anonymous reviewers that helped to improve our paper.

References

Amoakwah, E., Frimpong, K.A. & Arthur, E. 2017a. Corn cob biochar improves aggregate characteristics of a tropical sandy loam. *Soil Science Society of America Journal*, **81**, 1054–1063.

Amoakwah, E., Frimpong, K.A., Okae-Anti, D. & Arthur, E. 2017b. Soil water retention, air flow and pore structure characteristics after corn cob biochar application to a tropical sandy loam. *Geoderma*, **307**, 189–197.

Arthur, E., Tuller, M., Moldrup, P. & de Jonge, L.W. 2015. Effects of biochar and manure amendments on water vapor sorption in a sandy loam soil. *Geoderma*, **243–244,** 175-182.

Basso, A.S., Miguez, F.E., Laird, D.A., Horton, R. & Westgate, M. 2013. Assessing potential of biochar for increasing water-holding capacity of sandy soils. *GCB Bioenergy*, **5,** 132-143.

Blake, G. & Hartge, K. 1986. Particle density. *Methods of Soil Analysis: Part 1—Physical and mineralogical methods*(ed. A. Klute), pp. 377–382. SSSA Book Series 5.1. Soil Science Society of Ameria, America Society of Agronomy, Madison, WI.

Blanco-Canqui, H. 2017. Biochar and soil physical properties. *Soil Science Society of America Journal*, **81,** 687–711.

Bruun, E.W., Petersen, C.T., Hansen, E., Holm, J.K. & Hauggaard-Nielsen, H. 2014. Biochar

amendment to coarse sandy subsoil improves root growth and increases water retention. *Soil Use and Management*, **30,** 109–118.

Burrell, L.D., Zehetner, F., Rampazzo, N., Wimmer, B. & Soja, G. 2016. Long-term effects of biochar on soil physical properties. *Geoderma*, **282,** 96–102.

Cassel, D.K. & Nielsen, D.R.1986. Field capacity and available water capacity. In: *Methods of Soil Analysis: Part 1—Physical and Mineralogical Methods* (ed. A. Klute), pp. 901–926. SSSA Book Series 5.1. Soil Science Society of Ameria, America Society of Agronomy, Madison, WI.

Castellini, M., Giglio, L., Niedda, M., Palumbo, A.D. & Ventrella, D. 2015. Impact of biochar addition on the physical and hydraulic properties of a clay soil. *Soil & Tillage Research,* **154,** 1–13.

Chen, C., Hu, K., Li, W., Wang, G. & Liu, G. 2014. Estimating the wet-end section of soil water retention curve by using the dry-end section. *Soil Science Society of America Journal*, **78,** 1878–1883.

Christensen, B.T. 1986. Straw incorporation and soil organic matter in macro-aggregates and particle size separates. *Journal of Soil Science*, **37**, 125–135.

Cybulak, M., Sokolowska, Z. & Boguta, P. 2016. Hygroscopic moisture content of podzolic soil with biochar. *Acta Agrophysica*, **23**, 533–543.

Degens, B.P. 1997. Macro-aggregation of soils by biological bonding and binding mechanisms and the factors affecting these: a review. *Soil Research*, **35**, 431–460.

Devereux, R.C., Sturrock, C.J. & Mooney, S.J. 2012. The effects of biochar on soil physical properties and winter wheat growth. *Earth and Environmental Science Transactions of the*

Royal Society of Edinburgh. **103,** 13–18.

Du, Z., Wang, Y., Huang, J., Lu, N., Liu, X., Lou, Y. & Zhang, Q. 2014. Consecutive biochar application alters soil enzyme activities in the winter wheat–growing season. *Soil Science*, **179,** 75–83.

Du, Z., Zhao, J., Wang, Y. & Zhang, Q. 2017. Biochar addition drives soil aggregation and carbon sequestration in aggregate fractions from an intensive agricultural system. *Journal of Soils and Sediments*, **17,** 581–589.

Fungo, B., Lehmann, J., Kalbitz, K., Thionġo, M., Okeyo, I., Tenywa, M. & Neufeldt, H. 2017. Aggregate size distribution in a biochar-amended tropical Ultisol under conventional hand-hoe tillage. *Soil & Tillage Research*, **165,** 190–197.

Hardie, M., Clothier, B., Bound, S., Oliver, G. & Close, D. 2014. Does biochar influence soil physical properties and soil water availability? *Plant and Soil*, **376,** 347–361.

Khademalrasoul, A., Naveed, M., Heckrath, G., Kumari, K.G.I.D., de Jonge, L.W., Elsgaard, L. *et al*. 2014. Biochar effects on soil aggregate properties under no-till maize. *Soil Science*, **179**, 273–283.

Klute, A. & Dirksen, C. 1986a. Hydraulic conductivity and fiffusivity: Laboratory methods. In: *Methods of Soil Analysis: Part 1—Physical and Mineralogical Methods* (ed. A. Klute), pp. 687–734. SSSA Book Series 5.1. Soil Science Society of Ameria, America Society of Agronomy, Madison, WI.

Klute, A. & Dirksen, C. 1986b.Water retention: Laboratory methods. In: *Methods of Soil Analysis: Part 1—Physical and Mineralogical Methods* (ed. A. Klute), pp. 635–662. SSSA Book Series. 5.1. Soil Science Society of Ameria, America Society of Agronomy, Madison, WI.

Le Bissonnais, Y. 1996. Aggregate stability and assessment of soil crustability and erodibility: I. Theory and methodology. *European Journal of Soil Science*, **47,** 425–437.

Lehmann, J. 2007. A handful of carbon. *Nature*, **447,** 143-144.

Lehmann, J. & Joseph, S. 2015. Biochar for environmental management: an introduction. In: *Biochar for Environmental Management: Science, Technology and Implementation.* Second Edition (eds J. Lehmann & S. Joseph), pp. 1–14. Routledge, New York. NY.

Lim, T.J., Spokas, K.A., Feyereisen, G. & Novak, J.M. 2016. Predicting the impact of biochar additions on soil hydraulic properties. *Chemosphere*, **142,** 136–144.

Lu, F., Wang, X., Han, B., Ouyang, Z., Duan, X., Zheng, H. & Miao, H. 2009. Soil carbon sequestrations by nitrogen fertilizer application, straw return and no-tillage in China's cropland. *Global Change Biology*, **15,** 281–305.

Lu, S., Sun, F. & Zong, Y. 2014. Effect of rice husk biochar and coal fly ash on some physical properties of expansive clayey soil (Vertisol). *Catena*, **114,** 37–44.

Peng, X., Ye, L.L., Wang, C.H., Zhou, H. & Sun, B. 2011. Temperature- and duration-dependent rice straw-derived biochar: characteristics and its effects on soil properties of an Ultisol in southern China. *Soil & Tillage Research*, **112,** 159–166.

Petersen, C., Hansen, E., Larsen, H., Hansen, L., Ahrenfeldt, J. & Hauggaard‐Nielsen, H. 2016. Pore–size distribution and compressibility of coarse sandy subsoil with added biochar. *European Journal of Soil Science*, **67,** 726–736.

Qayyum, M.F., Steffens, D., Reisenauer, H.P. & Schubert, S. 2012. Kinetics of carbon mineralization of biochars compared with wheat straw in three soils. *Journal of Environmental Quality*, **41,** 1210–1220.

Rahman, M.T., Zhu, Q.H., Zhang, Z.B., Zhou, H. & Peng, X. 2017. The roles of organic amendments and microbial community in the improvement of soil structure of a Vertisol. *Applied Soil Ecology*, **111**, 84–93.

Rasband, W.S. 2007. ImageJ, US National Institutes of Health. Bethesda, MD, USA, *http://rsb. info. nih. gov/ij*, 1997-2016 (accessed 19 August 2018).

RStudio Team. 2015. *RStudio: Integrated Development for R.* RStudio, Inc., Boston, MA *URL* http://www.rstudio.com/ (accessed 19 August 2018).

Suliman, W., Harsh, J.B., Abu-Lail, N.I., Fortuna, A.-M., Dallmeyer, I. & Garcia-Pérez, M. 2017. The role of biochar porosity and surface functionality in augmenting hydrologic properties of a sandy soil. *Science of The Total Environment*, **574,** 139–147.

Sun, F. & Lu, S. 2014. Biochars improve aggregate stability, water retention, and pore-space properties of clayey soil. *Journal of Plant Nutrition and Soil Science*, **177,** 26–33.

Van Genuchten, M. T. 1980. A closed-form equation for predicting the hydraulic conductivity of unsaturated soils, *Soil Science Society of America Journal*, 44(5), 892-898.

Vogel, H.J. & Kretzschmar, A. 1996. Topological characterization of pore space in soil—sample preparation and digital image-processing. *Geoderma*, **73,** 23–38.

Wang, D., Fonte, S.J., Parikh, S.J., Six, J. & Scow, K.M. 2017. Biochar additions can enhance soil structure and the physical stabilization of C in aggregates. *Geoderma*, **303,** 110–117.

Zhou, H., Fang, H., Mooney, S.J. & Peng, X. 2016. Effects of long-term inorganic and organic fertilizations on the soil micro and macro structures of rice paddies. *Geoderma*, **266,** 66–74.

Table 1 Soil organic carbon (SOC), bulk density (ρ_b), soil particle density (ρ_s) and total porosity (ϕ) under no-biochar (CK), 4.5 (LB) or 9.0 t ha^{-1} year^{-1} biochar (HB), and straw return (SR) treatments.

Treatment	SOC/g kg^{-1}	ρ_b/g cm^{-3}	ρ_s/g cm^{-3}	ϕ/cm^3 cm^{-3}
CK	12.3	1.27	2.63	0.52
LB	19.8	1.22	2.60	0.53
HB	26.6	1.13	2.60	0.56
SR	14.1	1.24	2.61	0.52
SE	0.76	0.03	0.02	0.01
P value*	<0.001	0.007	0.188	0.011
LSD (5%)	2.41	0.09	–	0.04

SE, standard errors calculated from ANOVA; *testing the differences among treatments; *P* value of *F* ratio of treatment effect (degrees of freedom 3 and 6); LSD, least significant difference at $P < 0.05$.

Table 2 Soil macroporosity from CT imaging, saturated conductivity (K_s), field capacity (FC), permanent wilting point (PWP) and plant available water capacity (PAWC) under no-biochar (CK), 4.5 (LB) or 9.0 t ha^{-1} $year^{-1}$ biochar (HB), and straw return (SR) treatments.

Treatment	Macroporosity	K_s (cm h^{-1})	FC	PWP	PAWC
	/mm^3 mm^{-3}	/cm h^{-1}		/g g^{-1}	
CK	0.027	0.78	0.201	0.100	0.101
LB	0.027	0.59	0.224	0.108	0.116
HB	0.045	1.61	0.235	0.113	0.123
SR	0.053	0.82	0.215	0.103	0.112
SE	0.010	0.21	0.005	0.003	0.004
P value*	0.022	0.004	0.001	0.010	0.004
LSD (5%)	0.030	0.67	0.016	0.010	0.013

SE, standard errors calculated from ANOVA; *testing the differences among treatments, *P* value of *F* ratio of treatment effect (degrees of freedom 3 and 6); LSD, least significant difference at $P < 0.05$.

Figure captions

Figure 1 Effects of 8-year amendment of no-biochar (CK), 4.5 (LB) and 9.0 t ha^{-1} $year^{-1}$ biochar (HB), and straw return (SR) on (a) soil aggregate size distribution after dry sieving and (b) mean weight diameter (MWD) of 2–3- and 0.25–2-mm aggregates after wet sieving. Bars are standard errors calculated from ANOVA. The *P* represents *P* value of *F* ratio of treatment effect. The LSD represents the LSD value at significance $P < 0.05$

Figure 2 Effects of 8-year amendment of no-biochar (CK), 4.5 (LB) and 9.0 t ha^{-1} $year^{-1}$ biochar (HB), and straw return (SR) on the three-dimensional (3-D) pore structure. White colours indicate pores identified by X-ray microtomography.

Figure 3 Effects of 8-year amendment of no-biochar (CK), 4.5 (LB) and 9.0 t ha^{-1} $year^{-1}$ biochar (HB), and straw return (SR) on the soil pore-size distribution as quantified by X-ray microtomography. Bars are standard errors calculated from ANOVA. The *P* represents *P* value of *F* ratio of treatment effect. The LSD represents the LSD value at significance $P < 0.05$

Figure 4 Effects of 8-year amendment of no-biochar (CK), 4.5 (LB) and 9.0 t ha^{-1} $year^{-1}$ biochar (HB), and straw return (SR) on the wet range (0–1500 kPa) of the soil water retention curve. Bars are the LSD values at significance $P < 0.05$.

Figure 5 Effects of 8-year amendment of no-biochar (CK), 4.5 (LB) and 9.0 t ha^{-1} $year^{-1}$ biochar (HB), and straw return (SR) on the dry range (oven dryness–1500 kPa) of the soil water retention. Bars are the LSD values at significance $P < 0.05$ and LSD values were not shown if the treatment effect was not significant.

Figure 6 Effects of 8-year amendment of no-biochar (CK), 4.5 (LB) and 9.0 t ha^{-1} $year^{-1}$ biochar

(HB), and straw return (SR) on the slope (LS) of the dry range (oven dryness–1500 kPa) of the soil water retention curve. Bars are standard errors calculated from ANOVA. The *P* represents *P* value of *F* ratio of treatment effect. The LSD represents the LSD value at significance $P < 0.05$.

Figure 7 Relations between soil organic carbon (SOC) content and bulk density (a) and the slope (SL) of the dry range (oven dryness–1500 kPa) of the soil water retention curve (b).

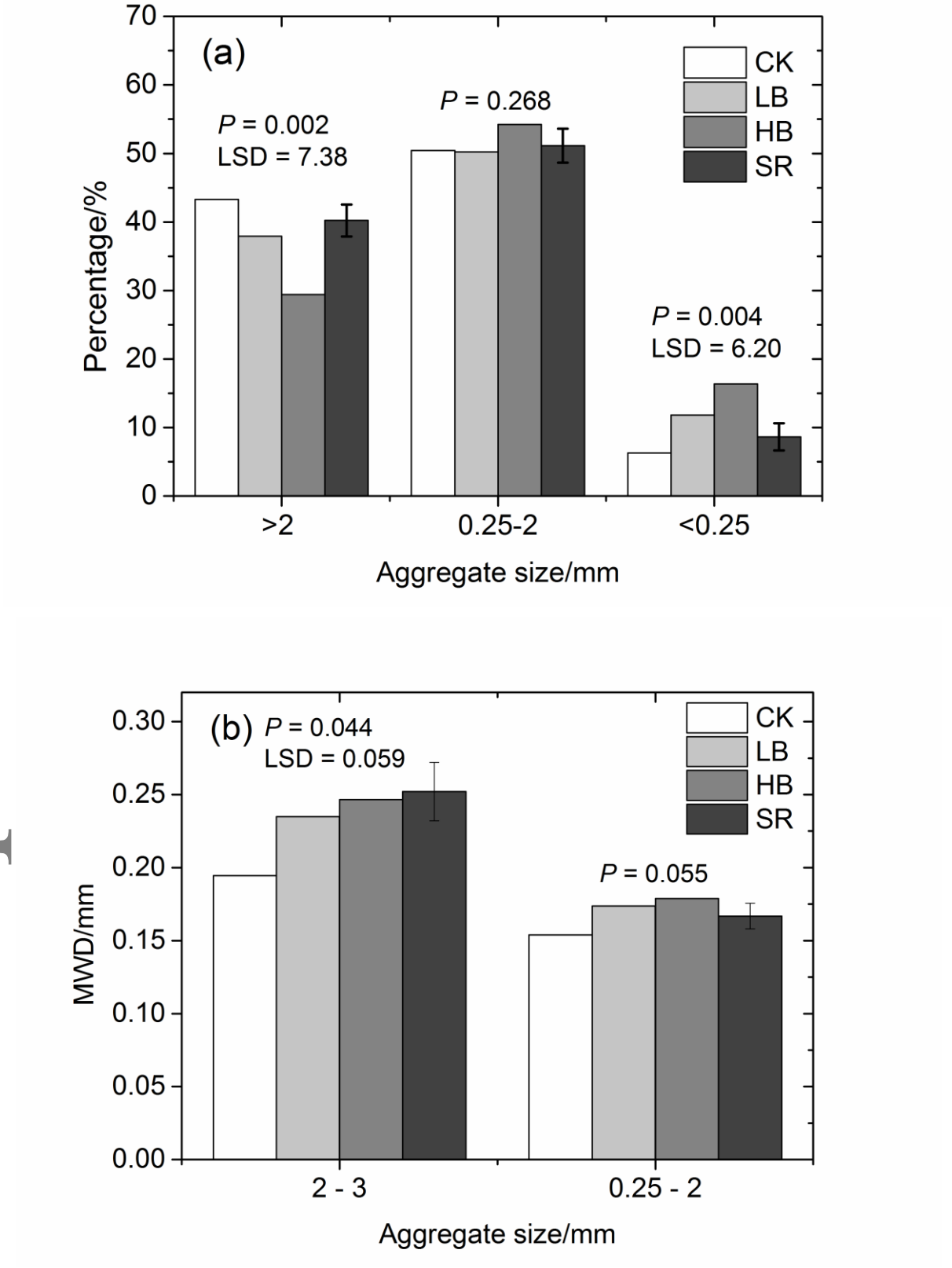

Figure 1

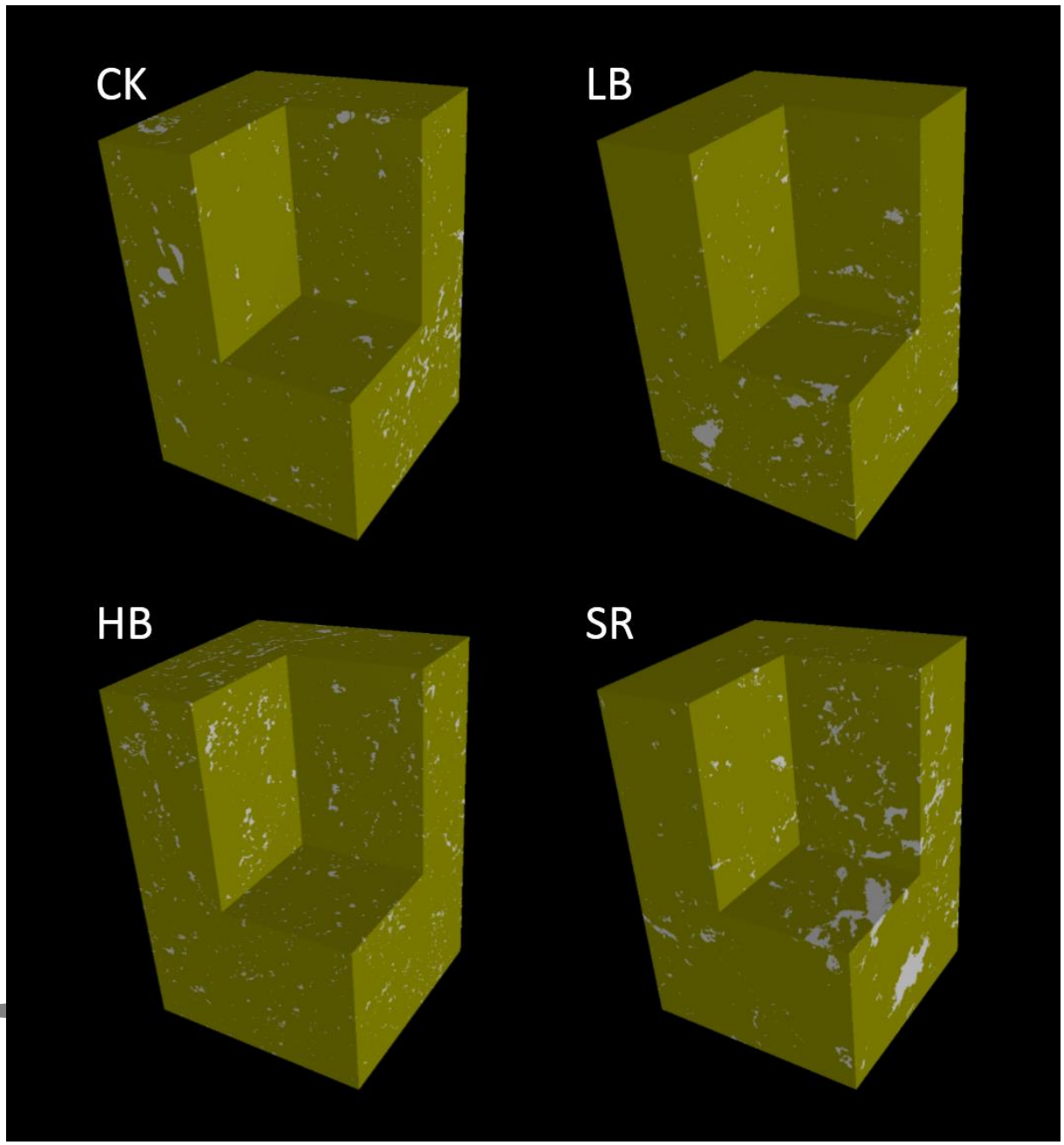

Figure 2

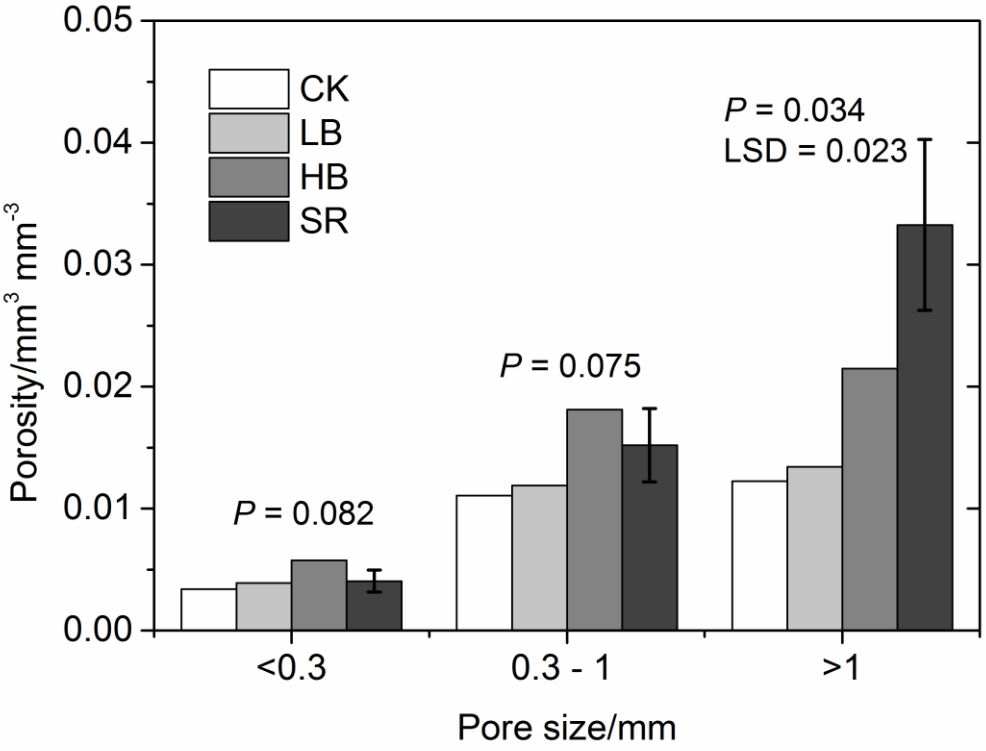

Figure 3

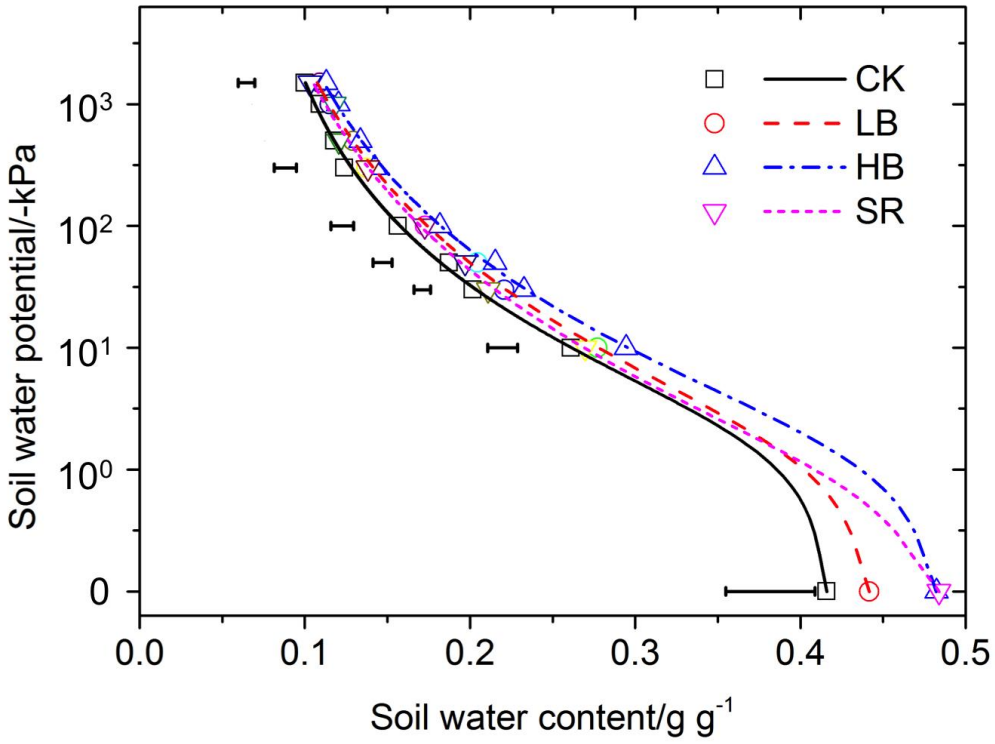

Figure 4

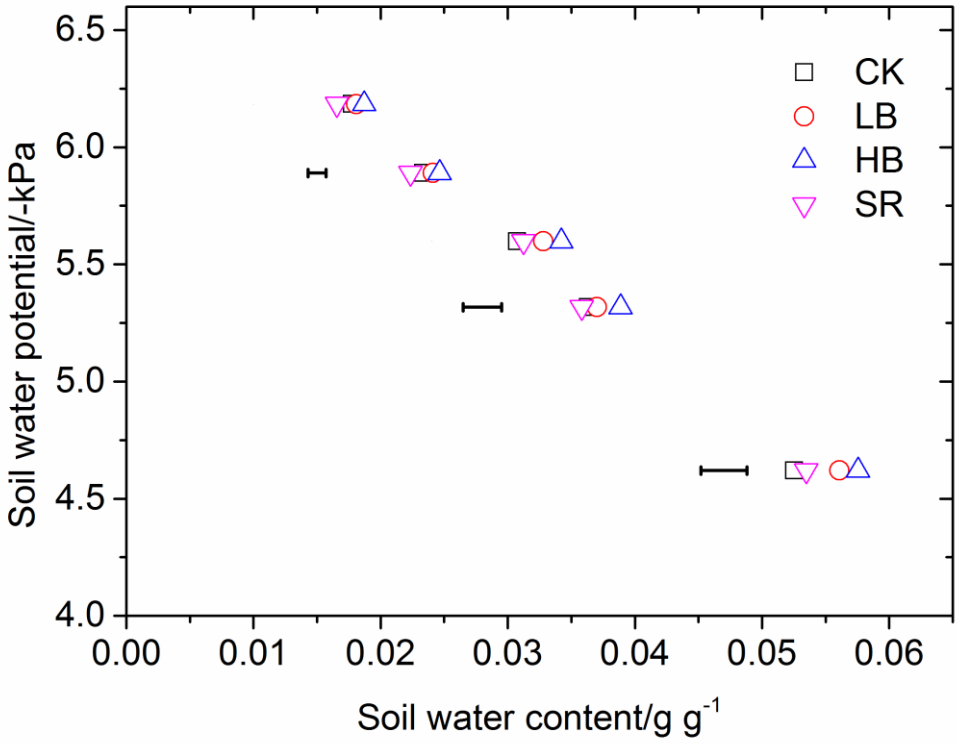

Figure 5

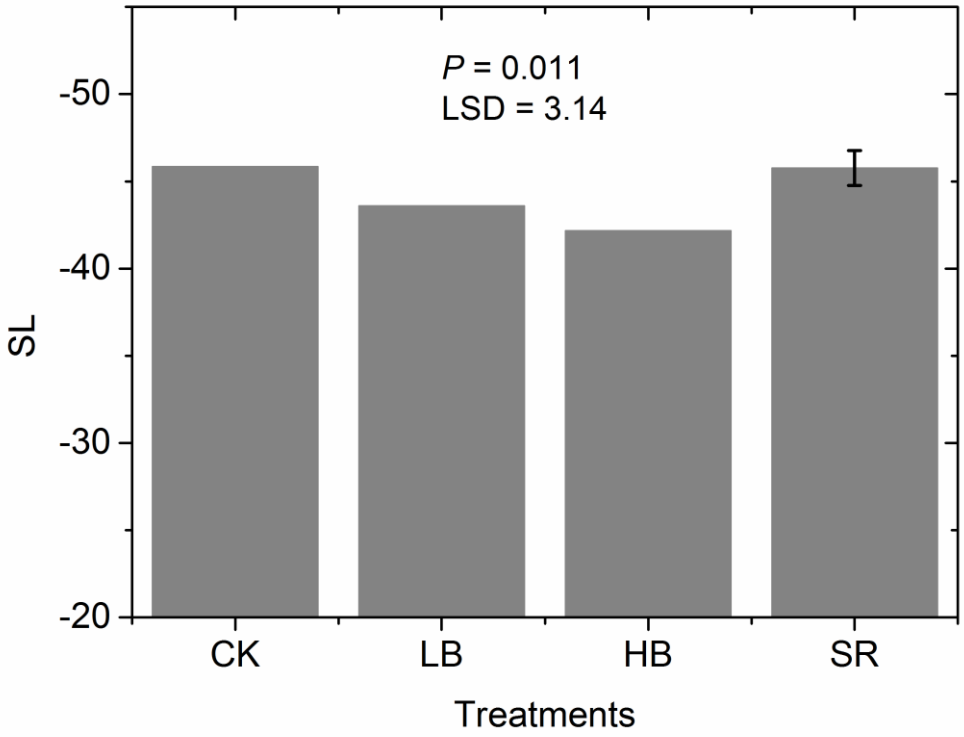

Figure 6

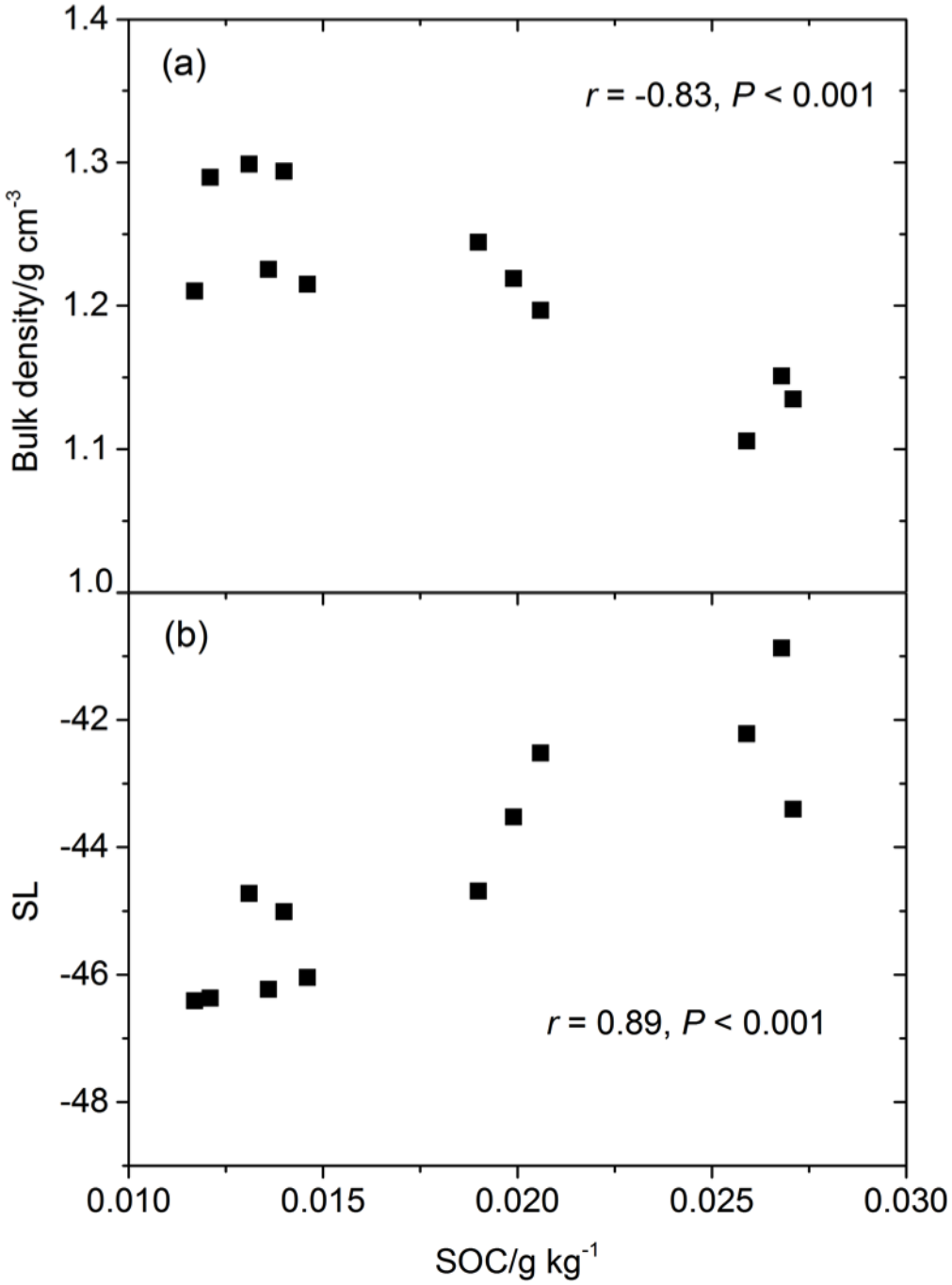

Figure 7